Journal of Alloys and Compounds 680 (2016) 43–53

Contents lists available at ScienceDirect

Journal of Alloys and Compounds

journal homepage: http://www.elsevier.com/locate/jalcom

Strain-energy transport during fracture of metallic glasses

J. Li [a], Y.W. Wang [a], J. Yi [a], I. Hussain [a], R. Li [b], B. Zhang [c], G. Wang [a, *]

[a] Laboratory for Microstructures, Institute of Materials, Shanghai University, Shanghai 200444, China
[b] School of Materials Science and Engineering, Beihang University, Beijing 100709, China
[c] School of Materials Science and Engineering, Hefei University of Technology, Hefei 230009, China

ARTICLE INFO

Article history:
Received 12 August 2015
Received in revised form
12 April 2016
Accepted 12 April 2016
Available online 14 April 2016

Keywords:
In-situ observation
DIC technique
Metallic glasses
Hyperelasticity model
Crack formation

ABSTRACT

In a strained metallic glass (MG), depending on its fracture toughness, the failure mode can be dominated by shear-banding failure (for tough MGs) or cracking failure (for brittle MGs). During the fracture process, crack formation and propagation create a nonlinear strain field at crack tip. The transportation of the strain energy stored in the strained MG to the crack tip is of importance in understanding the deformation mechanism of MGs. By using digital image correlation method, we perform direct and precise measurements of the strain concentration, including maximum strain value and the strain-energy distribution, in four MGs. After yielding, plastic deformation is localized into shear bands or crack tip in a scale of micrometer, which means a systematic transition from the linear elastic behavior to the strongly nonlinear behavior. Through quantitatively evaluating the balance between the fracture energy and the strain-energy density, the failure modes are discussed based on a hyperelasticity model. This result provides a comprehensive picture of how remotely applied forces drive MGs failure in the fundamentals of fracture states.

1. Background

Metallic glasses (MGs) without crystallographic defects acting as the plastic medium, usually have a high strength and a limited plasticity [1–3]. After the elastic deformation, some MGs with high toughness, such as Zr- and Cu-based MGs [4,5], yield through shear-band sliding, and some MGs with low toughness, such as Mg-based and La-based MGs [6,7], exhibit a macroscopic fracture without the activation of plastic yielding. Therefore, the relationship between the toughness and the plastic yielding via shear banding in MGs is of importance to understand elasto-plastic deformation mechanism. So far, most of work focus on the plastic mechanism, which generated numerous theories to quantitatively describe the deformation mechanism of MGs, such as the shear transformation zone (STZ) theory [8,9], the free volume theory [10], the flow units model [11,12], the liquid-like zone theory [13], and the geometrically unfavored motifs (GUMs) model [14] etc. Furthermore, the correlation between the fracture toughness and the elastic parameters of MGs was intensively studied to elucidate the deformation process [15–21]. However, the fracture of MGs is actually a process of a crack formation and propagation at a small scale [22]. The existence of a crack can dramatically amplify the external stress [23], in which a strain-concentration field is formed through a transportation of the externally applied elastic energy to the crack tip [24]. How the elastic energy transports in the shear-banding process of MGs, and how the elastic energy dissipates in the fracture process without plastically shear banding have not been well theoretically depicted because directly evaluating the elastic-energy accumulation is difficult. The key to understanding these questions may lie in the structure of the region in the front of the crack tip [25,26], where strains become so large that the linear elastic stress-strain response of MGs is already broken down.

Digital image correlation (DIC) technique provides an effective method to map the local displacement and the strain distribution on the sample's surface through the computation of a series of images recorded during the *in-situ* deformation [27,28]. Both a full-field visualization, and a dynamic evaluation of the strain are profiled simultaneously on a local level. The DIC technique has been previously applied to investigate the strain localization behavior, such as shear banding in MGs [29–31], whisker growth [32], crack growth in ceramics [33], damage measurement in rocks [34] etc. In these work, the DIC technique could accurately estimate the local strength of materials [35], locate the initiation place of micro-crack [36], and evaluate the maximum strain value for failure [37].

* Corresponding author.
E-mail address: g.wang@shu.edu.cn (G. Wang).

http://dx.doi.org/10.1016/j.jallcom.2016.04.117
0925-8388/

Accordingly, in this paper, four MGs, i.e., $Zr_{52.5}Cu_{17.9}Ni_{14.6}Al_{10}Ti_5$ (at.%), $Ce_{70}Ga_8Cu_{22}$, $Mg_{65}Cu_{25}Gd_{10}$ and $Co_{59}Ta_8B_{33}$ with different mechanical properties are chosen as the model materials. With the deformation evolving from an elastically stressing to a plastically yielding in MGs, a correlation between the strain-energy density and the fracture energy is observed to explain the failure modes.

2. Experimental procedure

The $Zr_{52.5}Cu_{17.9}Ni_{14.6}Al_{10}Ti_5$ and $Ce_{70}Ga_8Cu_{22}$ alloys were prepared by arc melting appropriate amounts of pure metal elements, with purities higher than 99.99%, in an argon atmosphere, and followed by suction casting into Cu-mould to form plate and rod samples. The $Mg_{65}Cu_{25}Gd_{10}$ metallic glass was prepared by induction melting plus injection casting. Cu—Gd pre-alloy was prepared by arc melting the mixture of pure metal elements in the argon atmosphere. A mixture of pure Mg element and Cu—Gd pre-alloy was induction melted under the argon atmosphere and then injected into a copper mould to form rod samples. The $Co_{56}Ta_9B_{35}$ glass rods were also prepared by induction melting casting. Co—B pre-alloy was prepared by arc melting the mixture of pure elements in the argon atmosphere. A mixture of pure Co, Ta element and Co—B pre-alloy were prepared by copper mould casting in the argon atmosphere to form rod samples. The diameter of the $Zr_{52.5}Cu_{17.9}Ni_{14.6}Al_{10}Ti_5$ (Zr-based MG), $Ce_{70}Ga_8Cu_{22}$ (Ce-based MG), $Mg_{65}Cu_{25}Gd_{10}$ (Mg-based MG) and $Co_{59}Ta_8B_{33}$ (Co-based MG) glassy rods were 2 mm.

The glassy phase structures of each cast specimen were examined by X-ray diffraction (XRD) in a Rigaku DLMAX-2550 diffractometer with the Cu-K_α radiation ($\lambda = 0.1542$ nm). The fractography of the fractured metallic glasses were observed with an APHENOM™ G2 (FEI company) scanning electron microscope (SEM). Compression specimens with a length/width (or length/diameter) ratio of 2 were cut from the rod samples. The ends of each specimen were carefully ground to a surface roughness of less than 1 μm. The rod samples were ground along the loading direction to be a half cylinder, as shown in the inset of Fig. 2a. After grinding, a surface of the cross-section with a size of 4 mm × 2 mm was shaped. In the center of the surface of the cross-section, a small area with a size of 2 mm × 1 mm (rectangular region covered by red color in the inset of Fig. 2a) was used for white digital speckle image correlation (DIC) method observation. Compression tests were conducted using an MTS CMT5205 machine at room temperature and a strain rate of 2.5×10^{-4} s^{-1}. For each MG, the compression tests were repeated four times to exclude the occasional results. The elastic parameters including elastic modulus, shear modulus, bulk modulus and shear wave speed were measured by the ultrasonic technique, for which an Olympus Panametrics NDT 5900PR ultrasonic testing device was used. The results are listed in Table 1. The stress intensity factor, K, measurements were carried out through using the circumferentially notched bar [17], which was estimated to be, $K = (0.526PD^{0.5})/d^2$, where D is the diameter of the rods used for the stress intensity factor (2 mm), P is the applied load, d is the diameter of circumferential notch, and $1.2 \leq D/d \leq 2.1$. The measured stress intensity factors of four MGs are listed in Table 1.

The strain field of the MGs' surfaces was observed by the DIC method. The surface of the sample was firstly spray-painted to generate artificial speckles and then illuminated by two fiber optic white light sources during loading. A CCD video camera (JAI CV-A1) was placed in front of the spray-painted surface to acquire the sequential speckle images necessary for performing digital speckle correlation. During the loading process, consecutive surface images were recorded with a 831 × 564 pixel CCD array and a length-pixel ratio of approximately 4.75 μm/pixel. The sequential images acquiring frequency was 4 Hz. A 211 × 422 pixel (1 × 2 mm) calculated domain was located at the middle of the sample. An image was obtained prior to loading that served as the reference (un-deformed) condition. The sequential images were analysed with respect to this reference condition using DIC, that can provide a displacement resolution in 0.01 subpixels, i.e., approximately 0.1 μm by a combination of the sub-pixel technique and the Newton-Raphson iteration algorithm. The strain distribution at different loads could then be identified by a series of pronounced contour maps. The DIC observation for each MG was repeated three times to confirm that the results were reproducible.

3. Results

Usually, the deformation behavior of MGs is seriously influenced by the microstructure of glassy phase. Especially, for the MGs with a relative low glass-forming ability, the microstructure of the glassy phase could be significantly changed during the quenching process. In the present study, the structures of four MGs were examined by XRD, which do not show any sharp diffraction peaks, confirming the glassy nature of four MGs (see Fig. 1). Therefore, the influence of the structure of the MGs on the mechanical tests can be ignored.

The nominal compression stress-strain curves of four MGs are plotted in Fig. 2. Their yield strength and plastic strain are listed in Table 1. The Zr-based MG shows the largest compressive ductility in the four MGs, which is manifested as a series of serrated events (Fig. 2a). The Ce-based MG shows a slightly plastic yielding after the

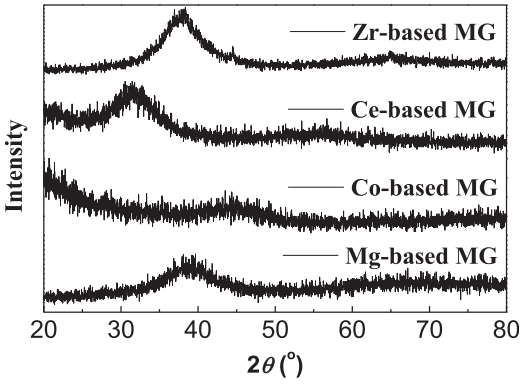

Fig. 1. XRD patterns of the four MGs.

Table 1
Mechanical properties of the four MGs, i.e., stress intensity factor (K), Poisson's ratio (ν), bulk modulus (B), shear modulus (G), Young's modulus (E), yield strength (σ_Y), plastic strain (ε_p), and shear wave speed (c_s).

Sample	K (MPa·m$^{0.5}$)	ν	B (GPa)	G (GPa)	E (GPa)	σ_Y (MPa)	ε_p	c_s (m/s)
Zr-based MG	42.6 ± 9.9	0.370 ± 0.009	114.1 ± 6.9	32.3 ± 0.9	88.6 ± 6.4	1749 ± 36	0.014 ± 0.003	2191 ± 39
Ce-based MG	5.7 ± 2.8	0.340 ± 0.012	31.8 ± 3.8	11.4 ± 1.2	30.5 ± 4.9	403 ± 21	0.014 ± 0.002	1277 ± 13
Co-based MG	5.0 ± 2.7	0.338 ± 0.011	248.2 ± 11.9	90.0 ± 1.5	240.1 ± 14.3	4763 ± 42	0.006 ± 0.002	3128 ± 9
Mg-based MG	1.3 ± 0.6	0.310 ± 0.013	45.1 ± 4.6	19.3 ± 1.0	50.6 ± 3.2	895 ± 29	0	2254 ± 11